Pure and Applied Geophysics

Numerical Simulation of Mesoscale Circulations in a Region of Contrasting Soil Types

SETHU RAMAN,[1] AARON SIMS,[1,2] ROBB ELLIS,[1] and RYAN BOYLES[1]

Abstract—Mesoscale processes that form due to changes in surface characteristics play a dominant role in the development of the planetary boundary layer structure and the formation of convection. In this study, effects of the Sandhills region of North and South Carolina on mesoscale processes are examined. Climatological analyses indicate increased convective precipitation in this location as compared to the surrounding region. This is believed to be due to enhanced convection induced by horizontal heat flux gradients caused by sharp changes in soil type and hence the heat capacity of the soil. Simulations using a non-hydrostatic mesoscale model (MM5 version 3.3) were made for a non-precipitation case with a 5-km resolution domain centered over the Carolinas from August 15, 2000 to August 18, 2000. The results showed the existence of a mesoscale circulation over the Sandhills region. Differential heating induced by contrasting soil types dividing the Coastal Plain from the central Piedmont causes this circulation. Sea-breeze circulation often combines with the Sandhills circulation to initiate convection in this region. Diurnal variations are handled well by the model indicating that the thermodynamic structure of the atmosphere is well simulated.

Key words: Mesoscale circulations, North Carolina, MM5, soil variation.

1. Introduction

Sandwiched between the Piedmont to the northwest and the Coastal Plain to the southest is an elongated area of sandy rolling hills in the Carolinas of the eastern United States called the Sandhills (Fig. 1). The adjacent Piedmont area contains primarily loam and clay-loam soils. These differing soil types exhibit varying characteristics such as drainage, albedo, and surface evaporation. It is the differences in the characteristics of these soil types that create differential heating of the earth surface. The heat capacity for sand is considerably less than that of clay or loam, so that given the same amount of energy, sandy soil would increase in temperature more than the loam or clay soils.

[1]State Climate Office of North Carolina, North Carolina State University, Raleigh, NC, 27695-7236, USA.
[2]Baron Advanced Meteorological Systems, Raleigh, NC 27695, USA.
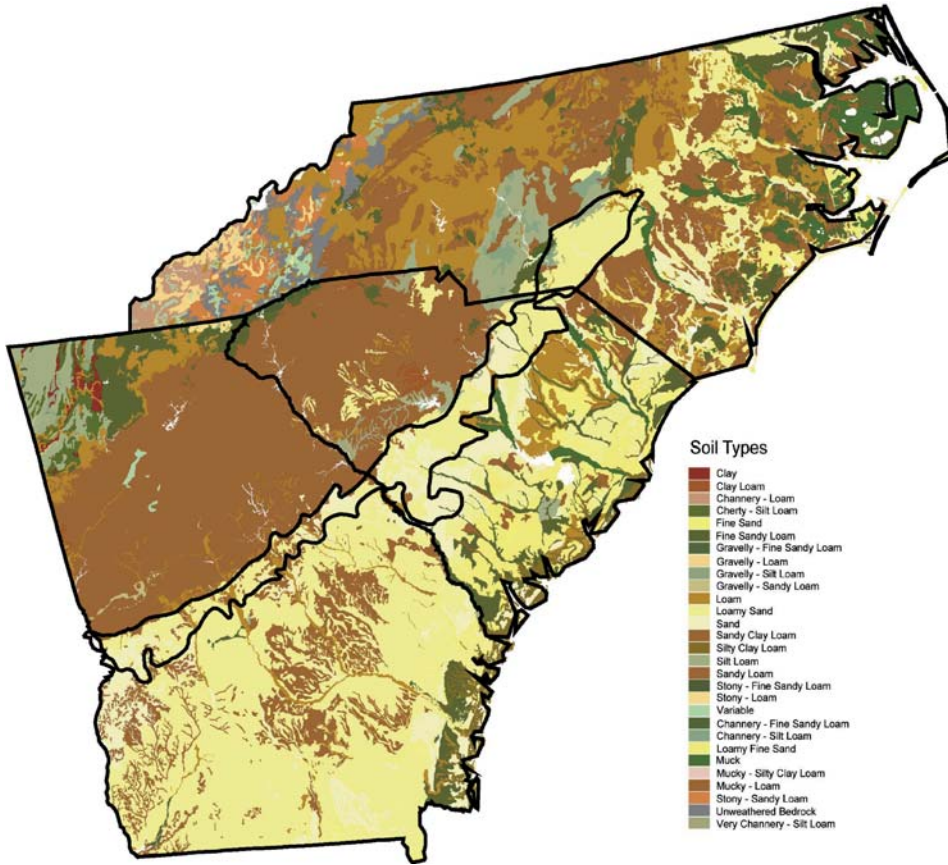
Figure 1
STATSGO-based soil types with Carolina Sandhills overlay.

The sea-breeze effect works in much the same way. The difference in the specific heats of water and land create differential heating. These differential surface heating patterns create mesoscale circulations causing clouds to form. Eventually, with the right large-scale conditions and the availability of moisture, thunderstorms form along the boundaries of these areas. Because surface heating is most intense during the summer months, these mesoscale convective processes are frequent during the months of June, July and August.

An elongated area of low pressure normally found at the transition from the Piedmont to the Coastal Plain during summers is characterized as the ''Piedmont Trough'' by KOCH and RAY (1997). It is believed that these areas of low-pressure form due to mesoscale convection created by intense heating of the surface. During their study of summertime mesoscale convective boundaries, KOCH and RAY (1997) noticed that this boundary existed for about 40% of the days. KOCH and RAY (1997)

explain that these boundaries are autoconvective, or produce convection without the interaction of any other boundaries such as sea-breeze fronts. When coupled with other types of boundaries they were found to be positively influential on convection. Any moisture associated with the coastal circulation or left by thunderstorms brought in by the sea breeze may have a positive effect on increased thunderstorm activity. They also found that the Sandhills region was second only to the sea-breeze front as a producer of the thunderstorms.

Climatological precipitation data for the month of July shown in Figure 2 indicate an increase over the Sandhills region in North Carolina and South Carolina. These data were gathered from over 200 cooperative observer sites in the Carolinas and Georgia for the period, 1960–1999. Also apparent in the figure is the effect of the sea breeze-associated precipitation and its inland extent.
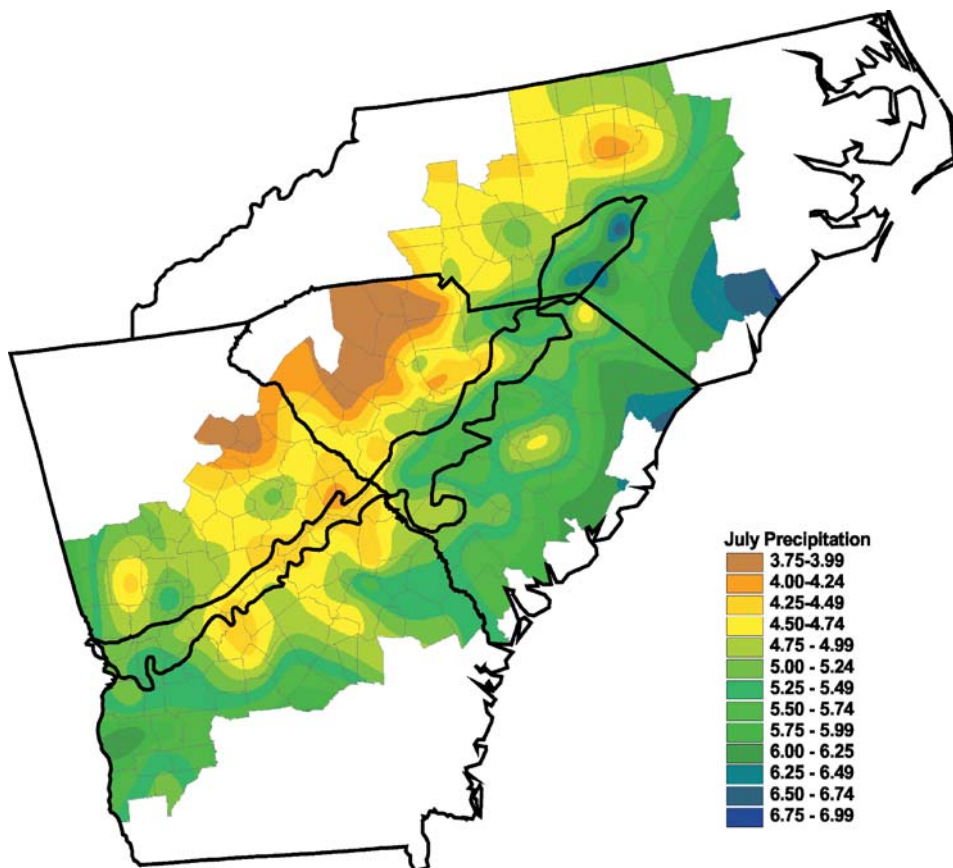

Figure 2
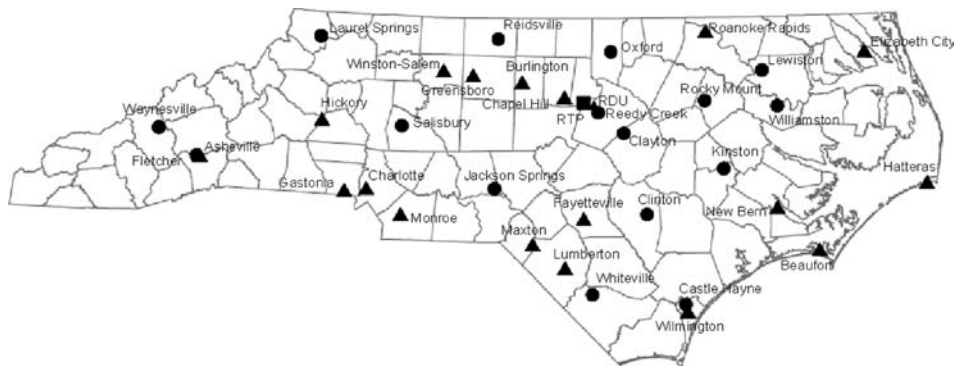Average of July precipitation in inches for the period 1960–1999.

Figure 3
Hourly surface observation stations across North Carolina. Triangle markers indicate ASOS stations. Circle markers indicate ECONet stations. The square marker indicates the location of the RTP SODAR station.

High-resolution observations across North Carolina (NC) provide valuable data to examine the accuracy of the MM5 modeling system. The hourly observation sites included ASOS (Automated Surface Observing System, operated by the National Weather Service) and NC ECONet (NC Environmental and Climate Observing Network, maintained by the State Climate Office of North Carolina) stations.

In the study reported here, numerical simulations of mesoscale processes and boundary layer structure over NC were performed. The combination of complex topography to the west, land-use pattern variations in the Piedmont, and close proximity to the coast in the east can cause significant mesoscale interactions and circulations. Analyses of modeled boundary layer processes and interactions are evaluated and validated with observed data. An examination of simulated horizontal and vertical cross sections in the 5-km domain is made. Additional analyses are performed to estimate model performance on a point-by-point basis. Thirty-six hourly surface observation stations across NC are shown in Figure 3. The relative locations of model grid points to observational sites are shown in Figure 4.

2. Numerical Model

Pennsylvania State University (PSU) and the National Center for Atmospheric Research (NCAR) developed the fifth generation mesoscale modeling system (MM5). Its design uses a terrain following a sigma coordinate system and a finite

▶

Figure 4
MM5 model grid for the 5-km domain overlaid on the hourly surface observation stations across North Carolina. Triangle markers indicate ASOS stations. Circle markers indicate AgNet stations. The square marker indicates the location of the SODAR station.
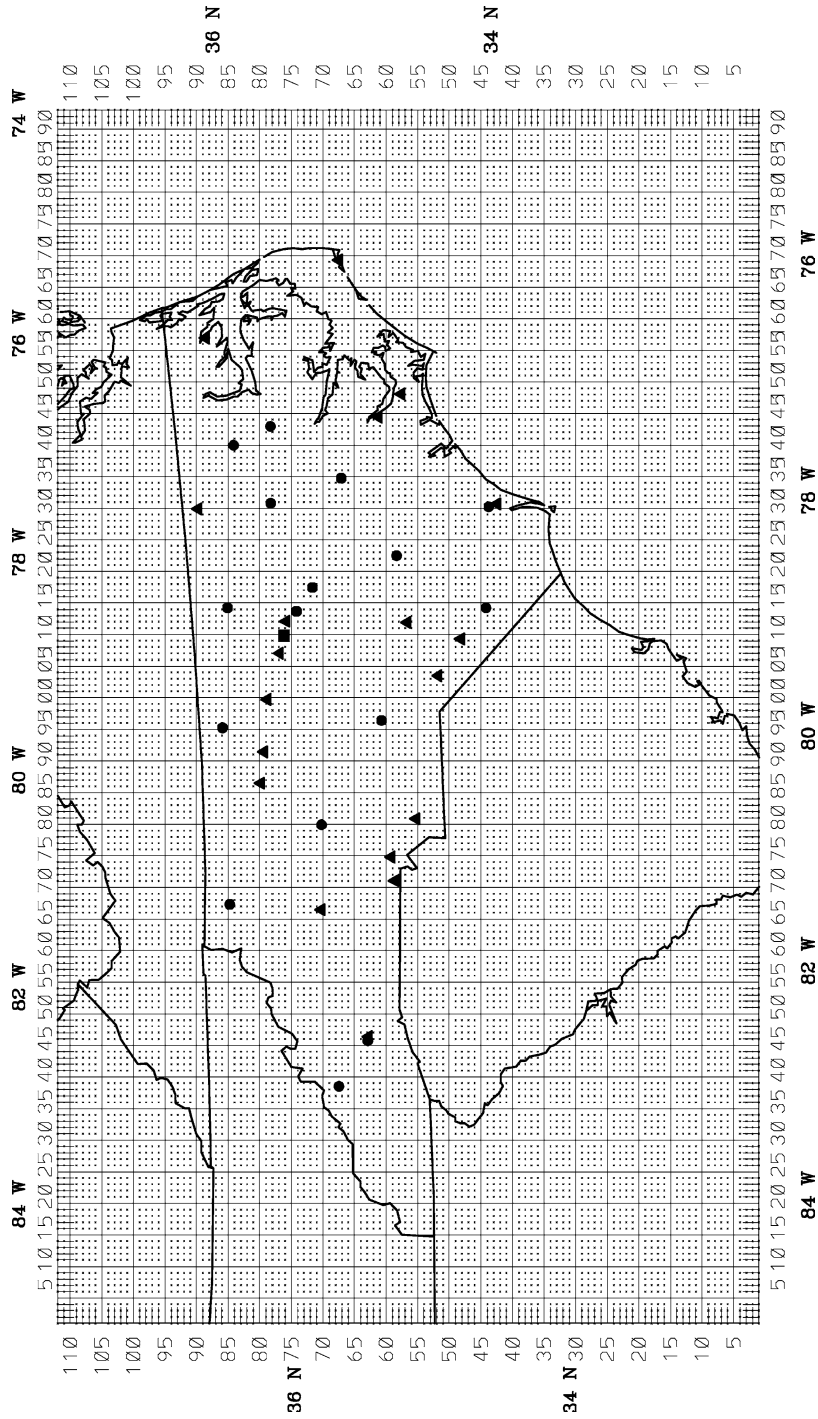
domain for the study of regional and mesoscale atmospheric phenomena. Version 3.3 of MM5 is used for the current study. Model simulations in this study use one-way nested domains. Nested grids employed in this simulation use a 3:1 coarse to fine grid resolution ratio. Boundary values for the coarse domain are derived from the analysis of the archived data set used in these simulations. Lateral boundary conditions are generated for the nested domain from the coarse domain simulation.

A triple nested domain configuration is used. The domain setup is shown in Figure 5. The coarse domain is centered at 36 degrees north and 85 degrees west and has a distance of 45 km between grid points. The number of grid points in the north-south direction is 54 and the east-west direction is 82. The second, intermediate domain has a resolution of 15 km with the number of east-west and north-south grid points totalling 112 and 76, respectively. The innermost domain has a resolution of 5 km. The grid points for this domain are 193 and 112 in the east-west and north-south directions, respectively.

Terrain and land-use data were obtained from the National Center for Atmospheric Research (NCAR). The terrain and land-use data for the innermost nested domain are shown in Figure 6. High-resolution elevation and land-use data were obtained from the United States Geological Survey (USGS). Additional data incorporated into the model also include soil type, vegetation fraction from AVHRR, and annual deep soil temperature from ECMWF analysis (GUTMANN and IGNATOV, 1998; USDA, 1994; ZOBLER, 1986). Soil types for the 5-km domain are shown in Figure 1.

All simulations use National Center for Environmental Prediction (NCEP) Global Data Assimilation System (GDAS) meteorological data obtained from the National Center for Atmospheric Research (NCAR). These data sets are archived at a resolution of 2.5 degrees every 12 hours (00Z and 12Z). These values were then interpolated to the model grid points.

The USGS land-use categories are shown in Table 1. In order to increase the boundary layer resolution, twenty-five of the total thirty-seven vertical levels are below 700 hPa. The cumulus parameterization scheme chosen for all simulations is the Kain-Fritsch (KF) scheme for its simplicity and ability to handle convection in small to medium grids (KAIN and FRITSCH, 1993; FRITSCH and CHAPPELL, 1980). This scheme simplifies the effects of cumulus convection by assuming all clouds in a model grid cell are of the same type and remain consistent while the clouds move through the specified grid cell. Regulation of convection is determined by a parcel's buoyant energy and the time it takes to remove that energy by convection. Moist convection occurs when low level forcing lifts air above the level of free convection (LFC). Vertical wind shear within the cloud layer affects precipitation efficiency. Cumulative effects of environmental compensation of subsidence as a result of updrafts and downdrafts affect the temperature and mixing ratio.

An explicit moisture scheme was also used in this study. MM5 has numerous such schemes including those for dry conditions, stable precipitation, warm rain
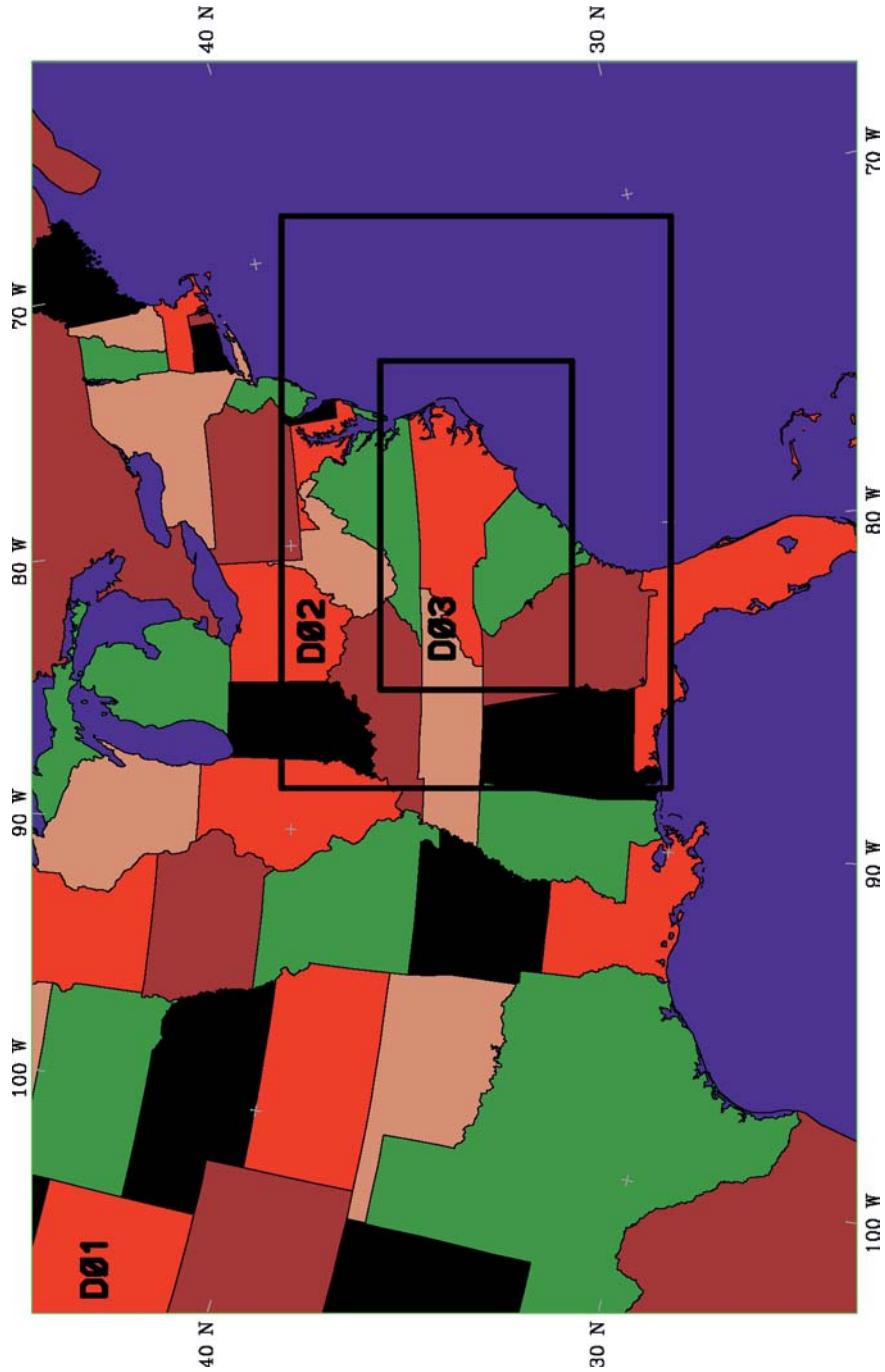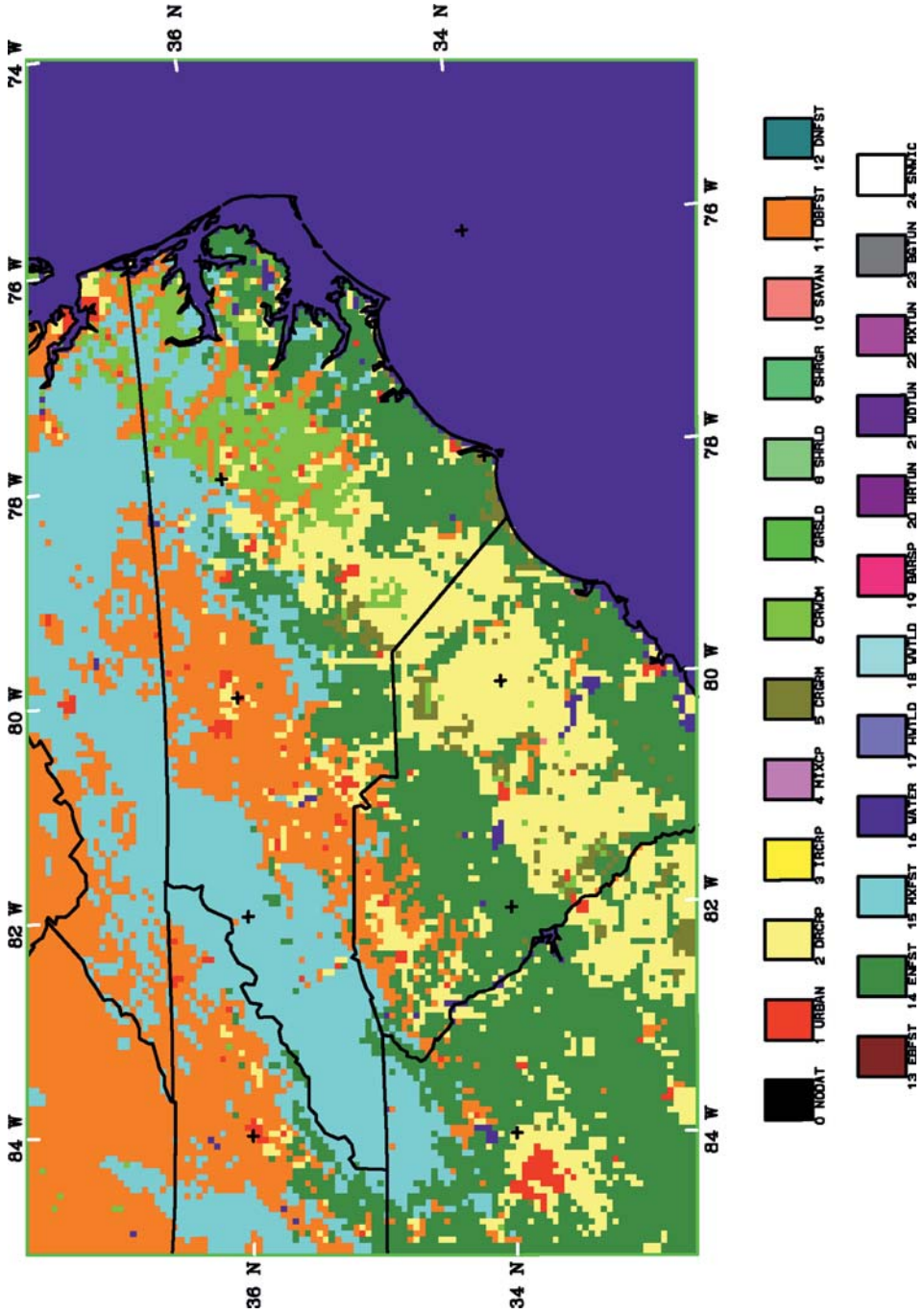
Figure 5
Domain setup centered over North Carolina.

Figure 6
Model dominant vegetation type / land use pattern.

Table 1

Vegetation Type and Land use Category

Category	Vegetation Type / Land Use
1	Urban and Built-Up Land
2	Dryland Cropland and Pasture
3	Irrigated Cropland and Pasture
4	Mixed Dryland/Irrigated Cropland and Pasture
5	Cropland/Grassland Mosaic
6	Cropland/Woodland Mosaic
7	Grassland
8	Shrubland
9	Mixed Shrubland/Grassland
10	Savanna
11	Deciduous Broadleaf Forest
12	Deciduous Needleleaf Forest
13	Evergreen Broadleaf Forest
14	Evergreen Needleleaf Forest
15	Mixed Forest
16	Water Bodies
17	Herbaceous Wetland
18	Wooded Wetland
19	Barren or Sparsely Vegetated
20	Herbaceous Tundra
21	Wooded Tundra
22	Mixed Tundra
23	Bare Ground Tundra
24	Snow or Ice

(KESSLER, 1969), simple ice (DUDHIA, 1989), mixed phase (LIN *et al.*, 1983), Goddard microphysics (TAO and SIMPSON, 1993), Reisner graupel (REISNER *et al.*, 1998), and Schultz microphysics (SCHULTZ, 1995). The simple ice scheme was chosen for its simplicity in these simulations.

The simple ice scheme handles moisture through several key assumptions. There is no super-cooled water in the simulation and ice crystals or snow immediately melt when crossing the zero degree isotherms. The assumption of no super-cooled water is based on the principle of the Bergeron-Findeisen process of ice crystals consuming available water droplets in elevations above the freezing level (DUDHIA 1989).

A cloud radiation scheme is used for these simulations. The scheme allows for longwave and shortwave radiation to interact with the clear air environment and explicit clouds. The longwave radiation calculations are based on the upward and downward fluxes determined by the effective emissivity, while absorption and scattering control calculations for the downward shortwave radiation (DUDHIA, 1989).

The MRF PBL (Medium Range Forecast Planetary Boundary Layer) scheme was chosen for simulations and is described by HONG and PAN (1996). Their effort is based on the boundary layer scheme developed by TROEN and MAHRT (1986). In this

scheme, similarity theory is used to represent the surface fluxes. Above the surface layer, mixing is represented by turbulent diffusivities based on bulk similarity and the stability conditions near the top of the surface layer.

3. Synoptic Conditions

The period, August 15, 2000 0000 (1900LST on August 14) through August 18, 2000 0000Z (1900LST on August 17), is a summer case with no precipitation. Throughout this period, synoptic winds were typically light and variable, allowing mesoscale features to influence the local weather. For most of the duration of this case study, high pressure dominated the southeast United States. Mild synoptic events in the case study include the passage of a dry trough of low pressure in western NC between 1200Z (0700LST) on the 16th and 0000Z (1900LST) on the 17th. Also, a dry, mild cold front passed through the domain between 0000Z (1900LST) and 1200Z (0700LST) on August 17 closely following this dry trough.

Cloud cover was minimal over the Carolinas during this case study. Some thin high cirrus clouds may have been present in the inner domain at times. An exception occurs during the last few hours of the period when heavier clouds begin to move into the domain from an approaching synoptic system.

4. Numerical Simulations

4.1 Soil Temperature and Soil Moisture

Observed and modeled soil temperature measurements are compared at a depth of 10 cm. Diurnal variations in soil temperature are handled well by the model in all regions. There appears to be less error in the modeled values during nighttime conditions. Nighttime observed point values of soil temperature are indicated in relation to the contours plotted from model values at 0600Z (0100LST) on August 16 as shown in Figure 7a. Here, the observations (provided in degrees K) match well with the simulated model values. In contrast, the daytime temperature comparison shown at 1800Z (1300LST) on August 16 in Figure 7b indicates large differences between the observed and modeled soil temperatures. In general, the model tends to overestimate the soil temperature at most locations by 3 to 5 degrees C during the daytime, possibly because of approximations and assumptions in the surface energy budget. A more complete statistical analysis of the simulated values is provided by SIMS (2001).

Modeled soil moisture is also compared with point observations from NC ECONet stations with available soil moisture data. The initial model soil moisture on August 15 at 0000Z (1900LST) is shown in Figure 8a. A fairly uniform distribution of approximately 0.33 m^3m^{-3} is apparent. Gradients in the modeled soil moisture develop during the simulation. Observed soil moisture values on August 15 at 1800Z
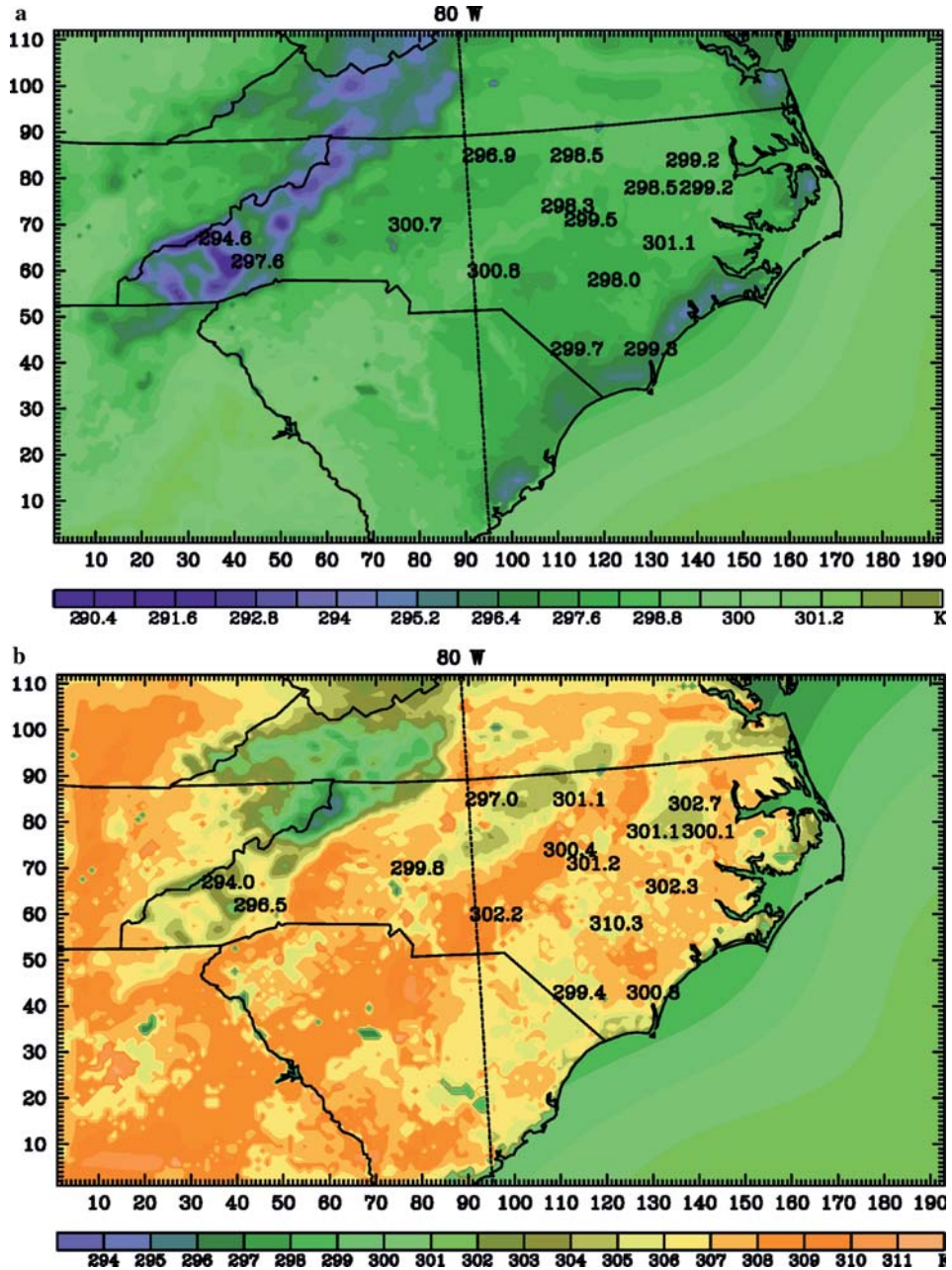
Figure 7a
Modeled soil temperature contours overlaid with actual observed soil temperature values obtained from NC ECONet stations in North Carolina at 0600Z (0100LST) on August 16, 2000 at 10 cm soil depth.

Figure 7b
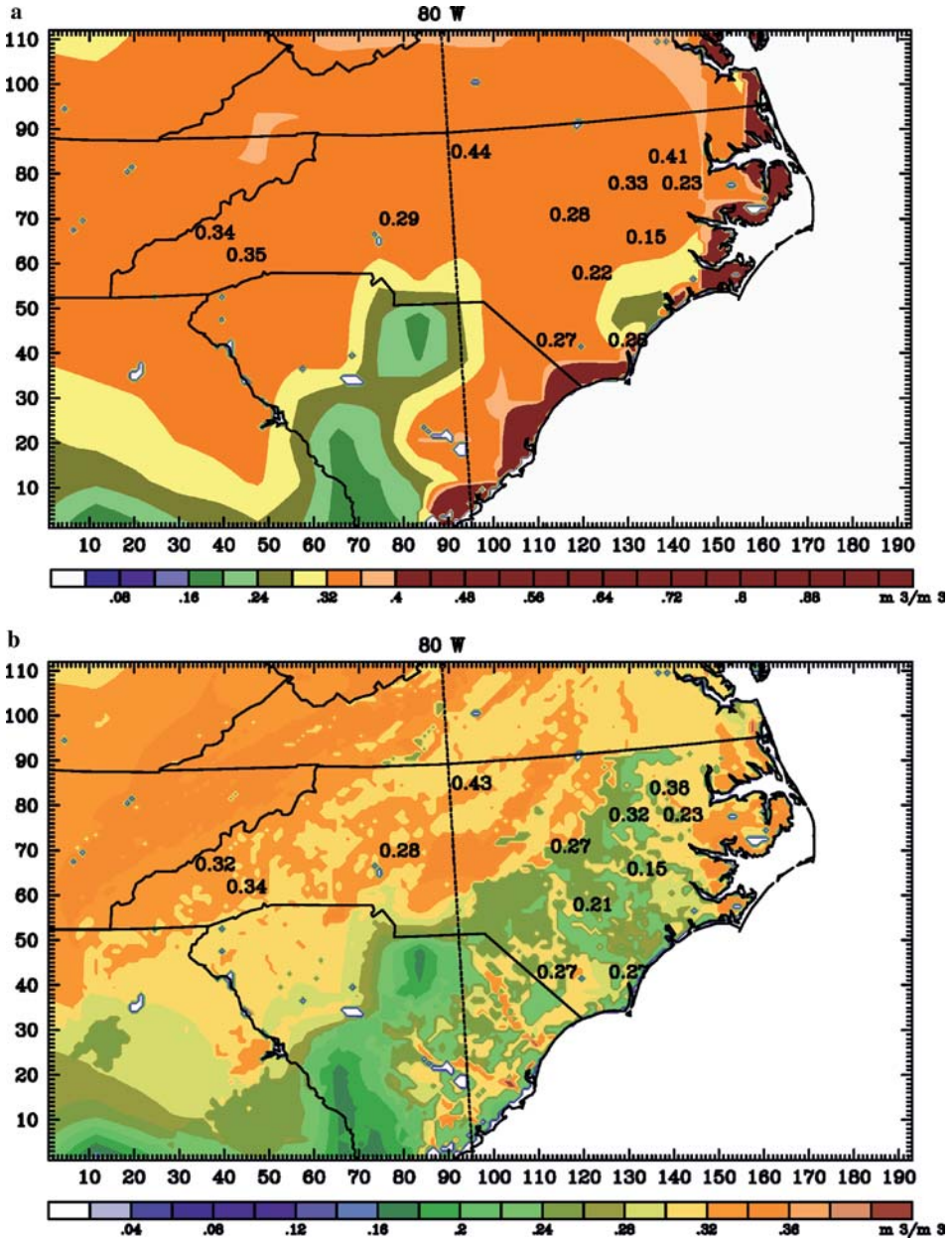As in Figure 5 except at 1800Z (1300LST) on August 16, 2000.

Figure 8a

Initial modeled soil moisture contours overlaid with actual observed soil moisture values obtained from NC ECONet stations in North Carolina at 0000Z (1900 LST) on August 15, 2000 at 10 cm soil depth. The initial field is noted to be fairly constant over North Carolina with a value of approximately 0.33 m^3/m^3.

Figure 8b

Modeled soil moisture contours overlaid with actual observed soil moisture values obtained from NC ECONet stations in North Carolina at 1800Z (1300 LST) on August 15, 2000 at 10 cm soil depth.

(1300LST) are then compared with model results by overlaying the observed values on the simulated soil moisture contours as shown in Figure 8b. A noticeable gradient in soil moisture is seen at the border of the Coastal Plain and Piedmont regions. This gradient is most likely caused by the difference in soil type and soil texture characteristics. Here, observations match well with the modeled soil moisture values. A drying of the sandy Coastal Plain is evident on August 17 at 1800Z (1300LST), as shown in Figure 8c, causing the soil moisture gradient between the Piedmont and Coastal Plain to increase over the Sandhills area. The modeled soil moisture in the Sandhills region has a value of approximately 0.20 m^3m^{-3}. The area adjacent to and west of the Sandhills still shows a soil moisture value of approximately 0.33 m^3m^{-3}.

In summary, soil moisture observations and model output are in good agreement. A noticeable gradient in soil moisture is seen at the border of the Coastal Plain and Piedmont regions due to the differences in the soil type and texture characteristics.

4.2 Sea Breeze Circulation

Simulated wind patterns for the inner domain are first analyzed using the horizontal wind vectors at the surface. Initial analysis of the wind vectors at 0000Z (1900LST) August 15 show a light northwesterly flow across much of the domain, with the strongest winds occurring offshore and over the northern Piedmont region of NC as indicated in Figure 9a.
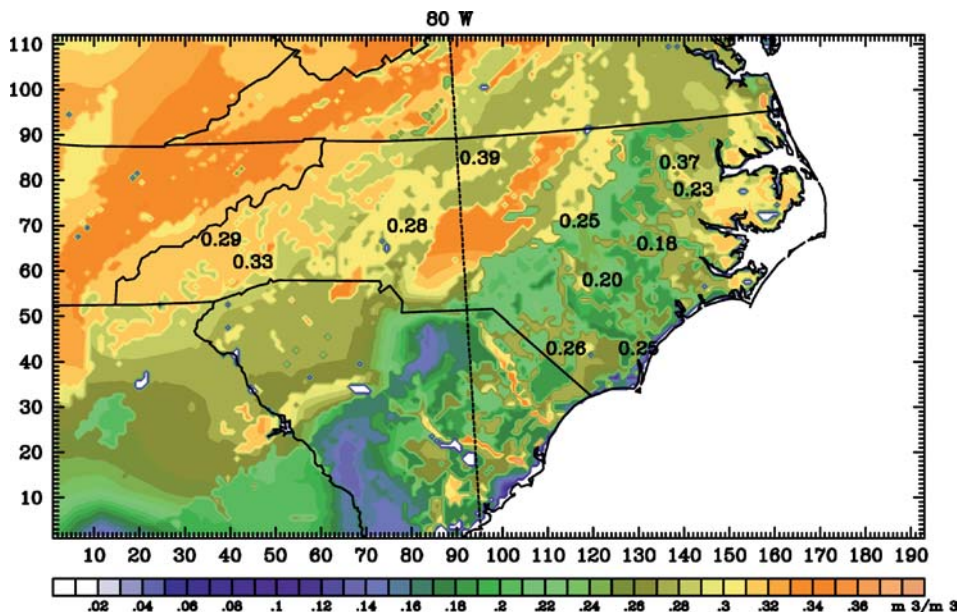

Figure 8c
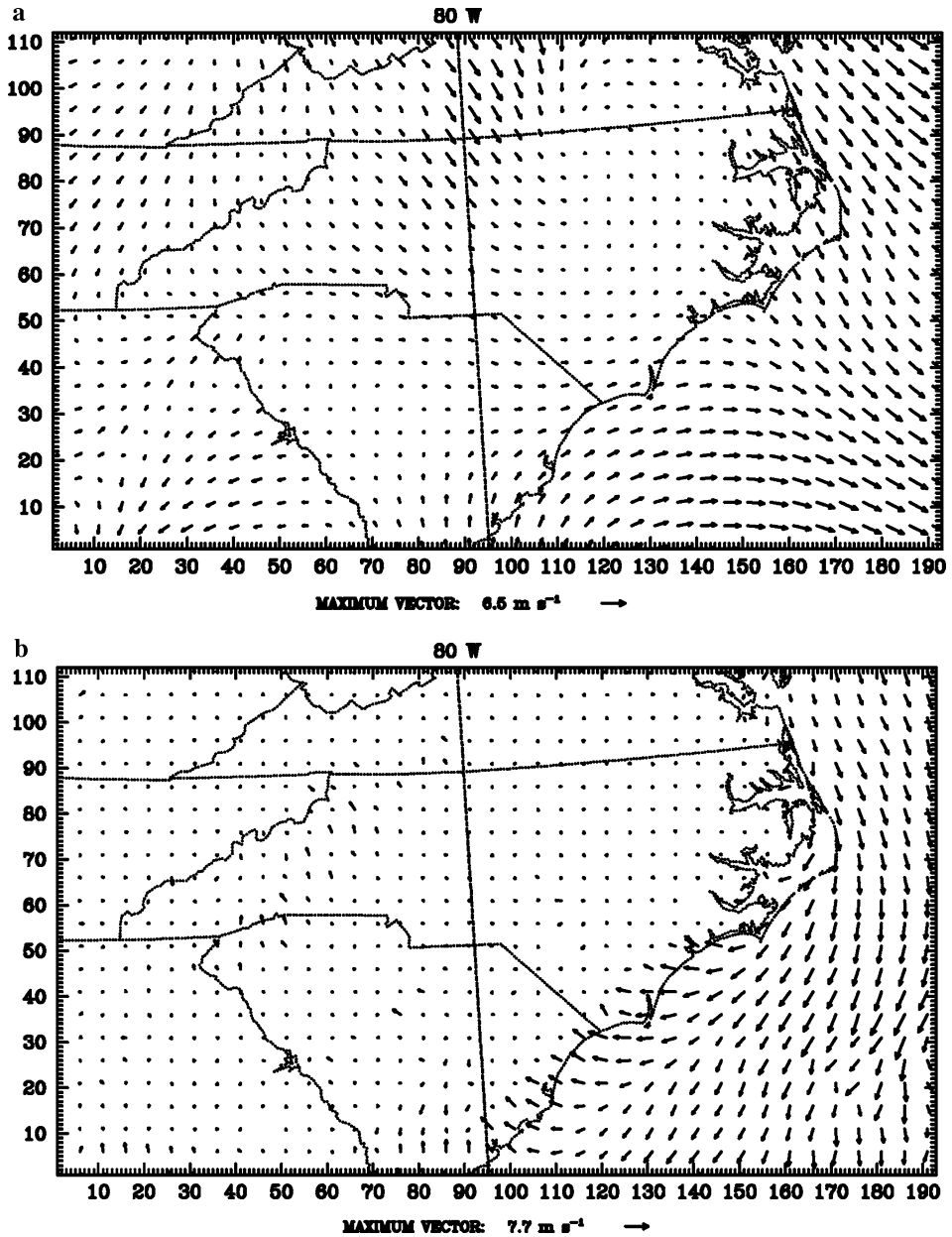As in Figure 8b except at 1800Z (1300 LST) on August 17, 2000.

a

b

Figure 9a
Horizontal wind vectors at 10 meters above the surface for the 5-km domain on August 15, 2000 at 0000Z
(1900LST).
Figure 9b
As in Figure 9a except at 1900Z (1400LST) on August 17, 2000.

Examination of the sea breeze development helps indicate how well the model simulates diurnal variation and differential heating. At 1900Z (1400LST) on August 15, 16, and 17, there is evidence of the development of a sea breeze indicated by a reversal of simulated surface winds towards the shore. An example of this wind reversal is shown in Figure 9b at 1900Z (1400LST) on August 17. Inland penetration of the sea breeze is approximately 30 km in the southern coastal region. To further determine the extent of the sea breeze, a cross section is taken along the southern coast of North Carolina near Wilmington; the location is indicated by the letter A in Figure 10. This cross section, shown in Figure 11 depicts a well-defined sea breeze circulation at 1800Z (1300LST) on August 15. Similar circulations were modeled on August 16 and 17 as well (not shown). The vertical extent of the simulated sea breeze circulation is approximately 500 m above the surface over the land-water boundary. The onset of the sea breeze was verified (not shown) using surface winds at 10 m height from Wilmington, Whiteville, Castle Hayne, Hatteras, and Beaufort (locations are indicated in Fig. 3).

4.3 Sandhills Circulation

Simulated wind vectors along cross section B across the Sandhills region of the Piedmont are shown in Figure 12. A well-defined circulation is evident in the simulation and extends well inland, to about 90 km over the Sandhills region. This region consists of a narrow band of sandy soil that borders the clay-based soils in the Piedmont as shown in Figure 1. Sharp contrasts in soil characteristics can result in
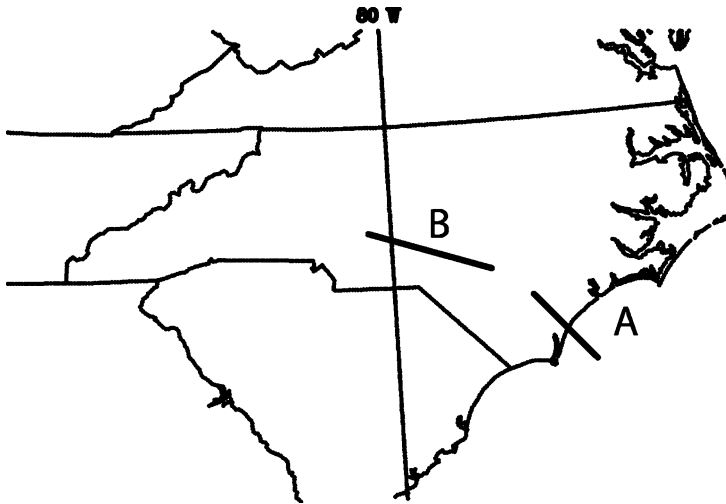

Figure 10
Lines A and B show the locations of the vertical cross sections. A is along the coast in North Carolina (NC) near the city of Wilmington. B is located across the Sandhills of NC.
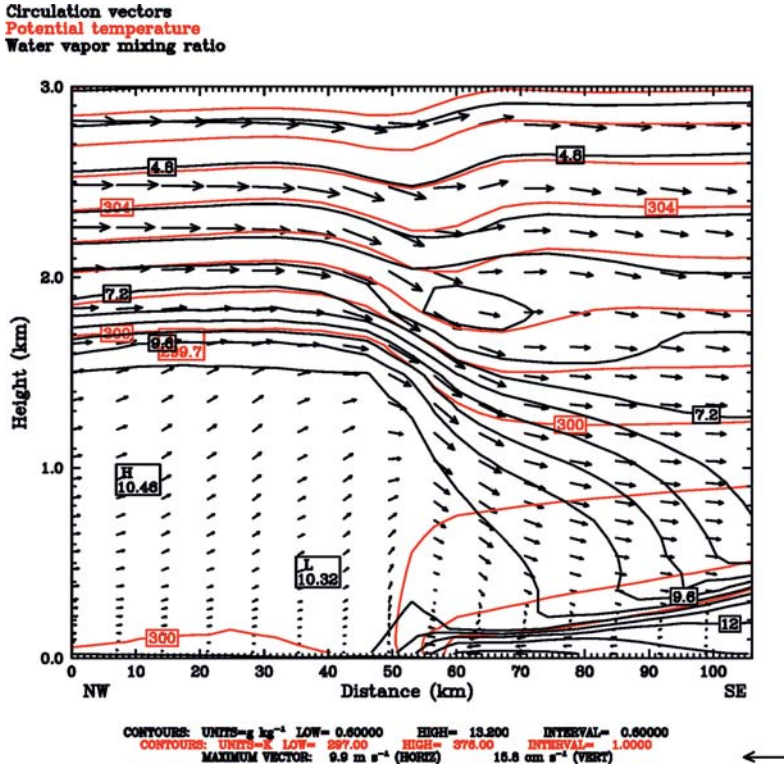
Figure 11

Vertical cross section showing circulation vectors (m/s), potential temperature (K), and water vapor mixing ratio (g/kg) for cross section A at 1800Z (1300LST) on August 15, 2000.

differential heating across this region. There is an area of convergence in the simulated Sandhills region where a strong southerly flow of about 6 m s^{-1} suddenly ceases in a narrow area of near calm winds. This convergence zone extends well into South Carolina and is oriented northeast to southwest.

Locally induced mesoscale circulations during the daytime hours in the Sandhills region at 0000Z (1900 LST) on August 18 is shown in Figure 13. The well developed circulation as seen at 0000Z (1900 LST) on August 18 horizontally extends approximately 70 km along the cross section and vertically extends of 2000 m.

There is a strong surface flow of about 4.6 m s^{-1} associated with this circulation as shown in Figure 13, with a strong upward component on the westward side of the circulation. Evolution of this feature over time produces a westward migration of this circulation feature whereby the center travels 35 km horizontally from east to west over a span of 6 hours. These circulations are not evident at 0600Z (0100 LST) on August 16 as shown in Figure 14. The flow in the early morning hours (0600 LST)
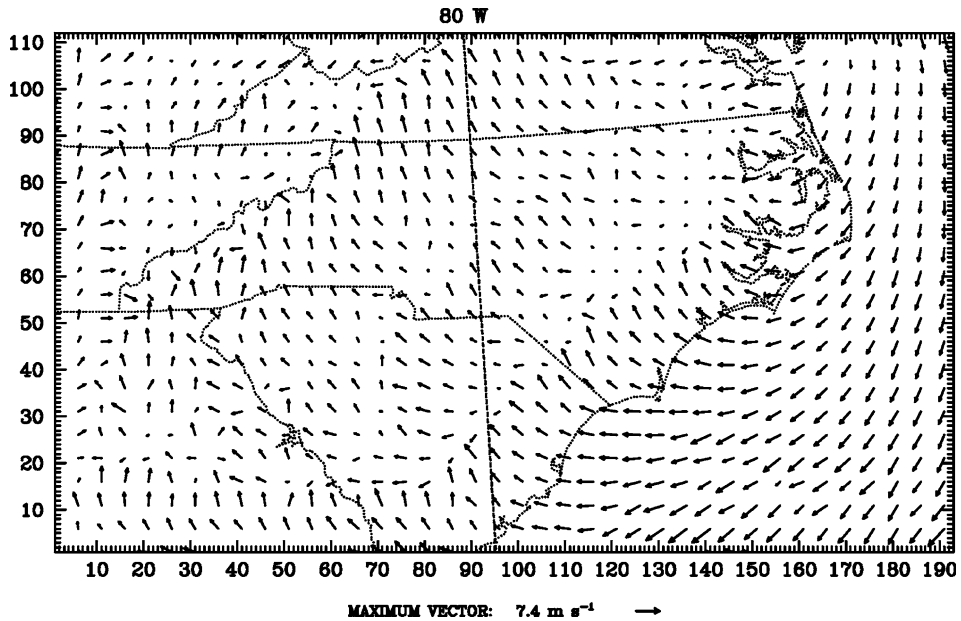
Figure 12
Surface wind vectors showing the formation of a Sandhills convergence zone inland at 0000Z (1900 LST) on August 18, 2000.

representative of nighttime conditions is fairly uniform and is from the west with a maximum wind speed of 4.3 m s^{-1}.

4.4 Planetary Boundary Layer Structure

Planetary boundary layer (PBL) heights were examined and compared with soundings from an upper air station at Greensboro (GSO), North Carolina. Also, SODAR data at the Environmental Protection Agency (EPA) site at a Research Triangle Park (RTP) location in North Carolina was obtained. This location is indicated in Figure 4 by a square marker on the map. Horizontal contour plots of PBL heights show significant diurnal variation with heights as low as 100 m at night and over 1500 m during the day. These variations are consistent with the overall observed variation. The simulated PBL heights at 1200Z (0700 LST) on August 15 are shown in Figure 15. Here, the simulated stable boundary layer over the innermost domain indicates an average height of approximately 200–300 m.

For this simulation period, SODAR observations were available at the Research Triangle Park in central Piedmont. PBL height variations on August 17 as observed by SODAR are shown in Figure 16 in which the solid line indicates the growth of the PBL with time. Modeled PBL heights at 1200Z (0700LST) are shown in Figure 17.
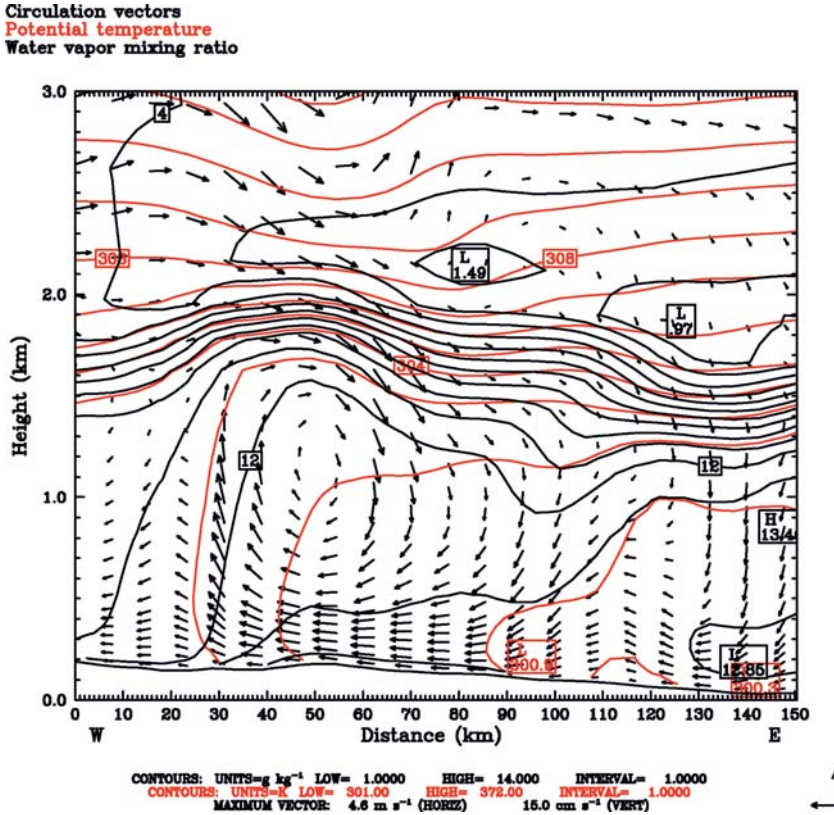
Figure 13

Formation of Sandhills circulation inland in the numerical simulation at 0000Z (1900 LST) on August 18, 2000. Initiation of convection generally takes place over this location.

The modeled PBL height at this time at the SODAR location is 300–400 m, while observations indicate a boundary layer height of about 200 m. Model overestimation was present at 1300Z (0800 LST) as well, where observations indicate a height of about 300 m while the model simulated a height near 400–500 m. Along the shore, modeled PBL growth in the coastal region is about 900 m. By 1400Z (0900LST), modeled heights near the SODAR location approached 800–900m, while observed heights were about 600 m.

The modeled PBL heights at 1500Z (1000LST) are approximately 1200 m to 1300 m at the SODAR location. The extent of the PBL height is not discernable by the SODAR at 1500Z (1000LST) because of range problems as shown in Figure 16. Based on the rate of growth as indicated in Figure 16, PBL heights were most likely at about 1000 m by this time. Along the coast, the model indicates PBL heights of approximately 1400 to 1500 m, whereas heights just offshore of the southern coast are still at 500 to 600 m.
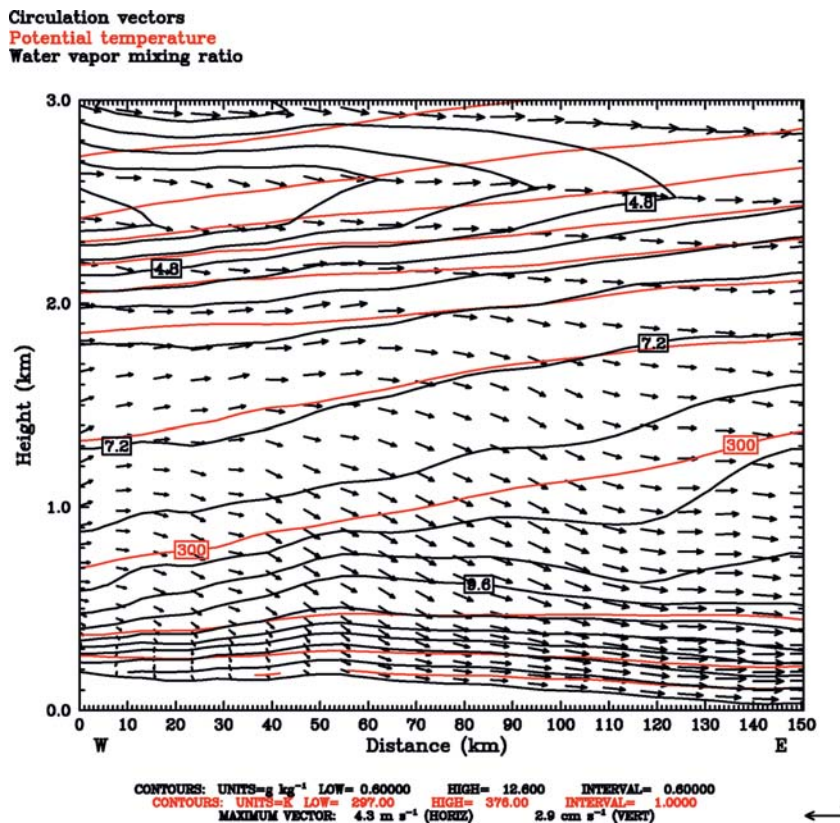
Figure 14

As in Figure 13 except at 0600Z (0100LST) on August 15, 2000. No circulation is seen in the simulation.

4.5 Land Surface Processes

Effects of heterogeneity in land use and soil types were evaluated with respect to the observed and the modeled land surface processes. Surface latent heat fluxes from the model simulation at 1800Z (1300 LST) on August 16 indicate a strong horizontal gradient in the Sandhills region as shown in Figure 18. A comparison of the location of this gradient with surface soil characteristics reveals a strong correlation of this latent heat flux gradient with the land use and soil type. Large latent heat fluxes, on the order of 500 Wm^{-2}, are present in the cropland area in conjunction with the loamy sand soil type. Reduced latent heat flux, about 350 Wm^{-2}, is simulated in the area adjacent to and just west of the Sandhills. The reduced latent heat flux appears to correlate with the finer grained soil and land cover change. Different field capacities for these soil textures combined with developing soil moisture gradients during the simulation may have contributed to these latent heat flux gradients in the Sandhills region. Another noticeable horizontal latent heat flux gradient is along the coast. The
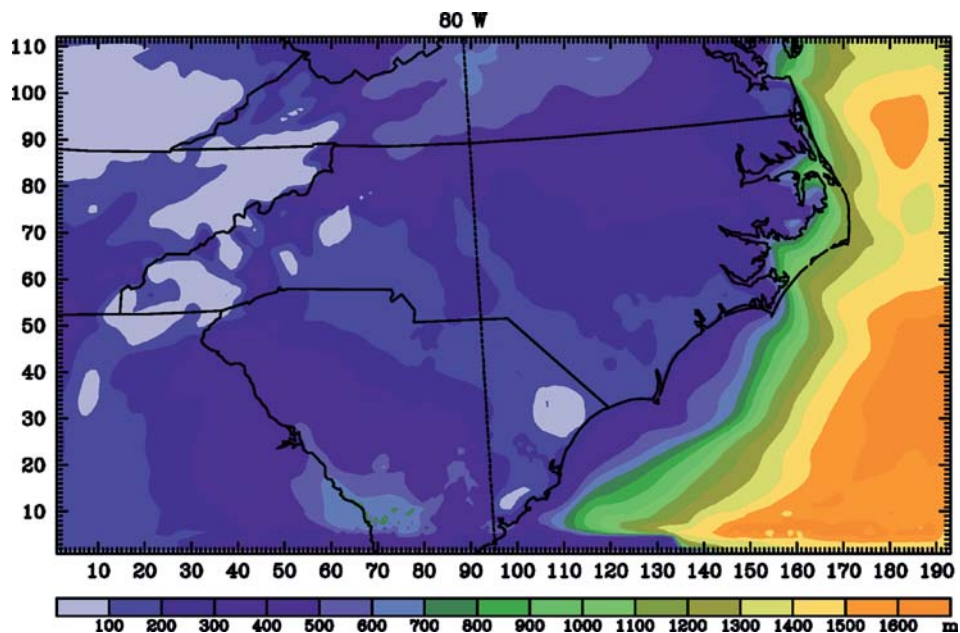
Figure 15
Planetary boundary layer heights for the 5-km domain on August 15, 2000 at 1200Z (0700LST).
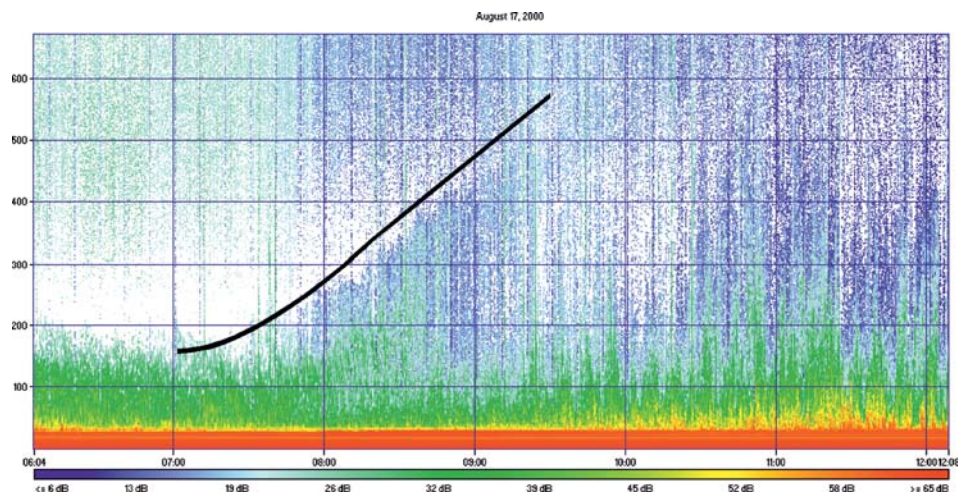

Figure 16
Color enhanced SODAR data obtained from the EPA near Research Triangle Park on August 17, 2000 from 1100Z to 1700Z (0600LST to 1200LST) showing the convective growth of the boundary layer.
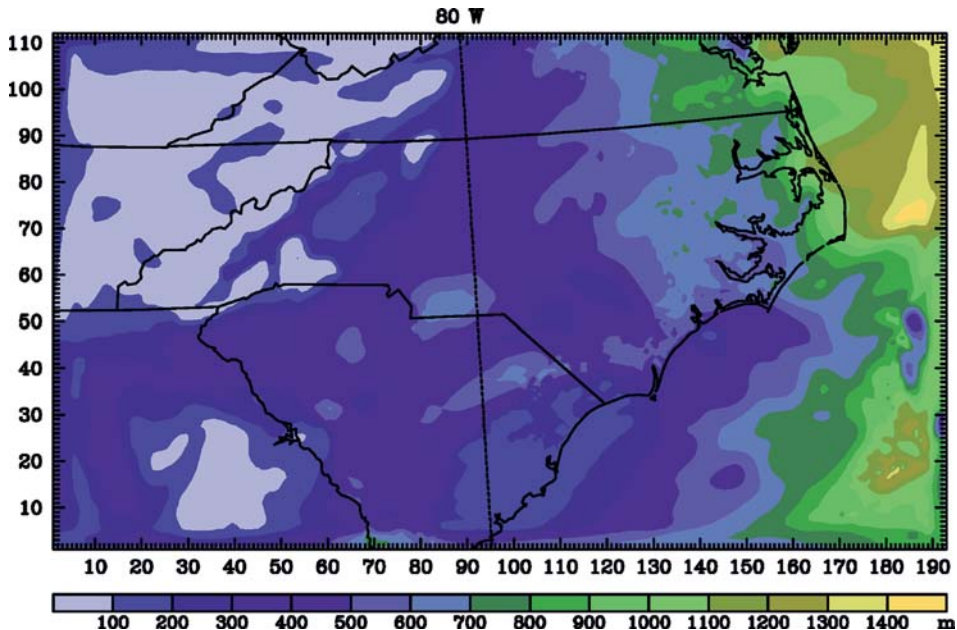
Figure 17
As in Figure 15 except on August 17, 2000 at 1200Z (0700LST).

simulated latent heat flux over land in the coastal region is approximately 400 Wm^{-2} and is larger than the flux over the coastal waters, of about 200 Wm^{-2}. The surface sensible heat flux distribution, shown in Figure 19 corresponds to the latent heat flux patterns at 1800Z (1300LST) on August 16. Sensible heat flux values decrease over the Sandhills region. This is possibly related to larger evapotranspiration occurring in this area as indicated by the larger latent heat fluxes as shown in Figure 18.

5. Evaluation of Simulated Surface Temperatures

Results from the time series comparison plots for stations at Wilmington (ILM) and Jackson Springs (JAC) are shown in Figures 20a and 20b, respectively. An overestimation of the nighttime temperatures by the model is apparent for both the locations. The station locations are indicated in Figure 3. This overestimation could be related to radiational cooling, as model performance tends to decrease in the day to night transitional period in which the observed rate of decrease in temperature exceeds the rate of decrease in temperature in the model. The overnight observational temperatures typically drop well below the modeled temperature by as much as 3 to 5 C (or K) at these locations. One possible cause is the error in the initial values of surface temperature and moisture.
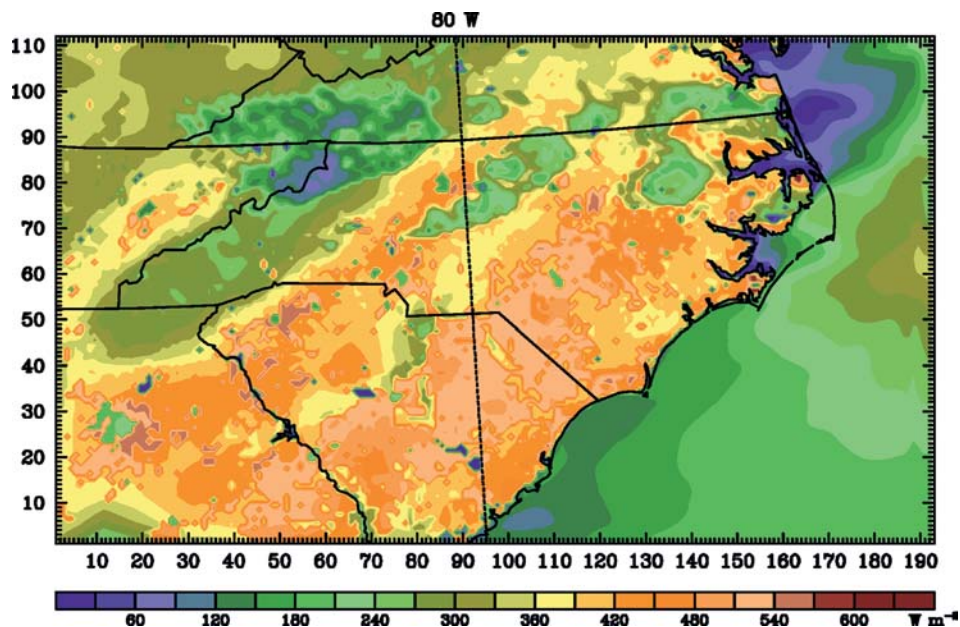
Figure 18
Latent heat flux (W m^{-2}) for the 5-km domain on August 16, 2000 at 1800Z (1300LST). A sharp gradient in the latent heat flux is seen in the central Piedmont near the Sandhills region.

During the night to day transitional period, the model quickly falls in line with the observations, handling the maximum temperatures well at most locations. Minor overestimations and underestimations of maximum temperature occur at roughly half the stations (SIMS, 2001).

6. Conclusions

During weak synoptic conditions, mesoscale processes can significantly impact regional weather. Examples of these processes include local surface heat flux gradients caused by differences in evaporation and transpiration from the earth's surface. Surface characteristics can also significantly contribute to the development of the planetary boundary layer and in turn virtually affect cloud and precipitation patterns. For example, soil moisture and texture and the land use affect surface characteristics, which in turn affects surface forcings. Correctly treating these land surface forcings is important for capturing and properly simulating terrain and land-use induced mesoscale circulations. Performance of a mesoscale model (MM5) was evaluated using surface observations, and SODAR measurements in North Carolina. Point-to-point comparisons of surface observations with the closest model grid point
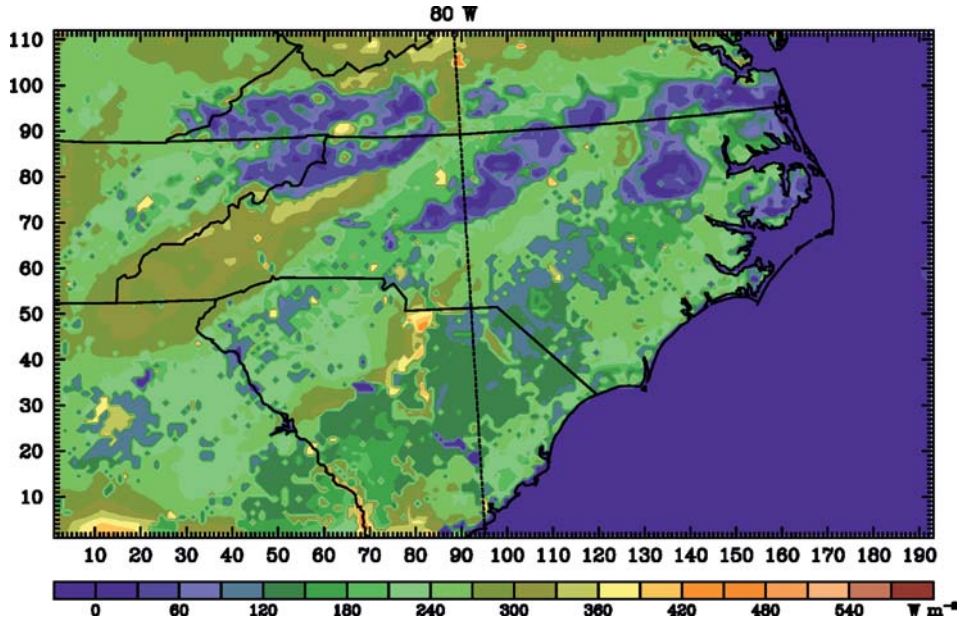
Figure 19
Sensible heat flux (W m^{-2}) for the 5-km domain on August 16, 2000 at 1800Z (1300LST). A sharp gradient in the sensible heat flux is seen in the central Piedmont near the Sandhills region.

values were performed using the 5-km model inner domain. Evaluation and validation of multiple surface parameters were performed.

The general flow patterns over the domain are well simulated by the model. The 5-km domain does simulate more mesoscale variability in the wind fields as compared to the 15-km outer domain. The model overestimates soil temperatures during daytime hours, especially in the Coastal Plain. The model simulates the soil moisture changes reasonably.

Observed nocturnal temperatures are cooler than the model predicted temperatures at the grid points closest to the observation stations. This problem could be due to improper representation, specification, and initialization of surface parameters including soil moisture, land use and texture as well as the surface energy budget. Diurnal variation of the boundary layer structure is well simulated. Nocturnal boundary layer heights appear to be simulated presentably by the model when compared with the soundings and the SODAR observations. The timing of the convective boundary layer growth also matches the observations well. The rate of growth, however, is somewhat overestimated by the model.

Magnitudes of the simulated latent and sensible heat fluxes vary depending on the land cover and soil type. Magnitudes of these heat fluxes depend on the soil moisture

a   **ILM Observed vs Forecasted Temperature**

b   **JAC Observed vs Forecasted Temperature**
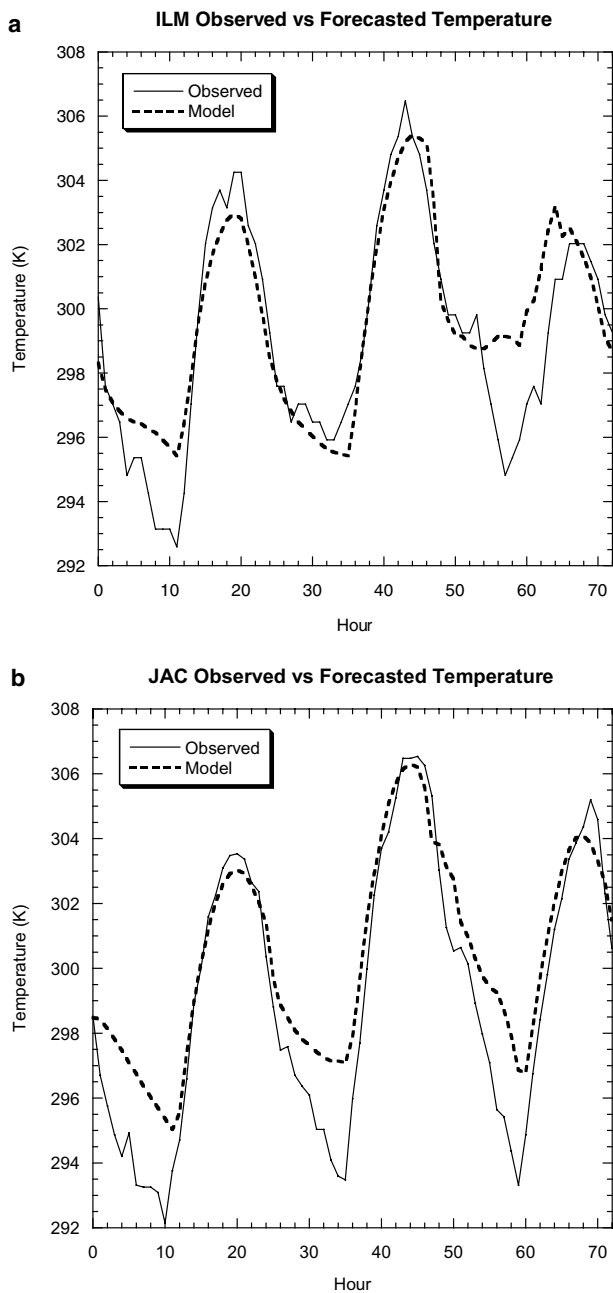
availability in the region and on the field capacity of the soil types. Significant horizontal gradients in the latent and sensible heat fluxes in the Sandhills region contribute to the development of mesoscale circulations observed in this region.

◄

Figure 20a

Observed and modeled air temperature at 2 m above the ground at Wilmington (ILM), NC. Forecast hours span 72 hours beginning at 0000Z (1900LST) on August 15, 2000 and ending on August 18, 2000 at 0000Z (1900LST). Modeled and observed temperatures are in and out of phase and match well during the daytime. The model overpredicts nighttime temperatures.

Figure 20b

As in Figure 18a except for the Jackson Springs (JAC) station.

Acknowledgements

REFERENCES

DUDHIA, J. (1989), *Numerical Study of Convection Observed during the Winter Monsoon Experiment Using a Mesoscale Two-dimensional Model,* J. Atmos. Sci. *46*, 3077–3107.

FRITSCH, J. M. and CHAPPEL, C. F. (1980), *Numerical Prediction of Convectively Driven Mesoscale Pressure Systems. Part I: Convective Parameterization,* J. Atmos. Sci. *37*, 1722–1733.

GUTMANN, G. J. and Ignatov, A. (1998), *The Derivation of Green Vegetation Fraction from NOAA/ AVHRR Data for Use in Numerical Weather Prediction Models,* Int. J. Remote Sens. *19,* 1533–1543.

HONG, S.-Y. and PAN, H.-L. (1996), *Nonlocal Boundary Layer Vertical Diffusion in a Medium-range Forecast Model,* Mon. Wea. Rev. *124,* 2322–2339.

KAIN, J. S. and FRITSCH, J.M., *Convective parameterization for mesoscale models: The Kain-Fritsch scheme.* In *The Representation of Cumulus Convection in Numerical Models,* (eds. Emanuel, K. A. and Raymond, D.J.) (Amer. Meteor. Soc. Boston 1993), 246 pp.

KESSLER, E. (1969), *On the Distribution and Continuity of Water Substance in Atmospheric Circulation,* Meteorol. Mon. Amer. Meteorol. Soc. *10*, 84.

KOCH, S. E. and RAY, K. A. (1997), *Mesoanalysis of Summertime Convergence Zones in Central and Eastern North Carolina,* Wea. and Forecasting *12*, 56–77.

LIN, Y.-L., FARLEY, R. D., and ORVILLE, H. D. (1983), *Bulk Parameterization of the Snow Field in a Cloud Model,* J. Climate Appl. Meteor. *22*, 1065–1092.

REISNER, J., RASMUSSEN, J., and BRUINTJES, R.T. (1998), *Explicit Forecasting of Supercooled Liquid Water in Winter Storms Using the MM5 Mesoscale Model,* Quart. J. Roy. Meteor. Soc. *124B*, 1071–1107.

SCHULTZ, P. (1995), *An Explicit Cloud Physics Parameterization for Operational Numerical Weather Prediction,* Monthly Wea. Rev. *123*, 3331–3343.

SIMS, A., *Effect of Mesoscale Processes on Boundary Layer Structure and Precipitation Patterns: A Diagnostic Evaluation and Validation of MM5 with North Carolina ECONet observations* (North Carolina State University, Raleigh 2001) 219 pp.

TAO, W.-K. and SIMPSON, J. (1993), *The Goddard Cumulus Ensemble Model, Part 1: Model Description,* Terr. Atmos. Oceanic Sci. *4*, 35–72.

TROEN, I. and MAHRT, L. (1986), *A Simple Model of the Atmospheric Boundary Layer: Sensitivity to Surface Evaporation,* Bound. Layer Meteor. *37*, 129–148.

USDA *State Soil Geographic (STATSGO) Data Base* (U.S Department of Agriculture, Natural Resources Conservation Service, Miscellaneous Publication 1492, 1994).

ZOBLER, L., *A world soil file for global climate modeling* (NASA Tech. Memo. 87802, 1986) [Available from NASA Goddard Space Flight Center, Institute for Space Studies, 2800 Broadway, New York, NY 10025.]